



**HAL**  
open science

## Subcellular localization of microcystin in the liver and the gonads of medaka fish acutely exposed to microcystin-LR

Qin Qiao, Chakib Djediat, H el ene Huet, Charlotte Duval, S everine Le Manach, C ecile Bernard, Marc Edery, Benjamin Marie

### ► To cite this version:

Qin Qiao, Chakib Djediat, H el ene Huet, Charlotte Duval, S everine Le Manach, et al.. Subcellular localization of microcystin in the liver and the gonads of medaka fish acutely exposed to microcystin-LR. *Toxicol*, 2019, 159, pp.14-21. 10.1016/j.toxicol.2018.12.006 . mnhn-02293039

**HAL Id: mnhn-02293039**

**<https://mnhn.hal.science/mnhn-02293039>**

Submitted on 27 Sep 2019

**HAL** is a multi-disciplinary open access archive for the deposit and dissemination of scientific research documents, whether they are published or not. The documents may come from teaching and research institutions in France or abroad, or from public or private research centers.

L'archive ouverte pluridisciplinaire **HAL**, est destin ee au d ep ot et  a la diffusion de documents scientifiques de niveau recherche, publi es ou non,  emanant des  tablissements d'enseignement et de recherche fran ais ou  trangers, des laboratoires publics ou priv es.

1 **Subcellular localization of microcystin in the liver and the gonads of medaka fish**  
2 **acutely exposed to microcystin-LR**

3 *Qin Qiao<sup>1</sup>, Chakib Djediat<sup>1</sup>, H  l  ne Huet<sup>1,2</sup>, Charlotte Duval<sup>1</sup>, S  verine Le Manach<sup>1</sup>,*  
4 *C  cile Bernard<sup>1</sup>, Marc Edery<sup>1</sup>, Benjamin Marie<sup>1,\*</sup>*

5 <sup>1</sup> UMR 7245 MNHN/CNRS Mol  cules de Communication et Adaptation des  
6 Micro-organismes, Sorbonne Universit  s, Mus  um National d'Histoire Naturelle, CP  
7 39, 12 Rue Buffon, 75005 Paris, France.

8 <sup>2</sup> Ecole Nationale V  t  rinaire d'Alfort, Universit   Paris-Est, BioP  le Alfort, 94700  
9 Maisons-Alfort, France.

10

11 \* Corresponding author. UMR 7245 MNHN/CNRS Mol  cules de Communication et  
12 Adaptation des Micro-organismes, Sorbonne Universit  s, Mus  um National  
13 d'Histoire Naturelle, CP 39, 12 Rue Buffon, 75005 Paris, France. Tel.: +33 1 40 79 32  
14 12

15 E-mail address: bmarie@mnhn.fr (B. Marie)

16

17 **Abstract**

18 Among the diverse toxic components produced by cyanobacteria, microcystins  
19 (MCs) are one of the most toxic and notorious cyanotoxin groups. Besides their potent  
20 hepatotoxicity, MCs have been revealed to induce potential reproductive toxicity in  
21 various animal studies. However, little is still known regarding the distribution of  
22 MCs in the reproductive organ, which could directly affect reproductive cells. In order  
23 to respond to this question, an acute study was conducted in adult medaka fish (model  
24 animal) gavaged with 10  $\mu\text{g}\cdot\text{g}^{-1}$  body weight of pure MC-LR. The histological and  
25 immunohistochemical examinations reveal an intense distribution of MC-LR within  
26 hepatocytes along with a severe liver lesion in the toxin-treated female and male fish.  
27 Besides being accumulated in the hepatocytes, MC-LR was also found in the  
28 connective tissue of the ovary and the testis, as well as in oocytes and degenerative  
29 spermatocyte-like structures but not spermatocytes. Both liver and gonad play  
30 important roles in the reproductive process of oviparous vertebrates. This observation

31 constitutes the first observation of the presence of MC-LR in reproductive cells  
32 (female, oocytes) of a vertebrate model with *in vivo* study. Our results, which provide  
33 intracellular localization of MC-LR in the gonad, advance our understanding of the  
34 potential reproductive toxicity of MC-LR in fish.

35 **Keywords:**

36 Microcystin; reproductive cell; immunogold electron microscopy; OATP;  
37 reproductive toxicity

38

39 **1. Introduction**

40 Recurrent cyanobacterial blooms frequently occur worldwide in eutrophic  
41 freshwaters. Various bloom-generating species of cyanobacteria can produce natural  
42 toxic components (cyanotoxins), and their blooms threaten human health as well as  
43 living organisms of the aquatic environment. Among cyanotoxins, microcystins (MCs)  
44 are the most prevalent cyanobacterial hepatotoxins, with 248 structural variants  
45 (Spoof and Catherine, 2017), being produced by at least six genera of cyanobacteria  
46 (Puddick et al., 2014). Among all these known variants, microcystin-LR (MC-LR) is  
47 considered to be the most common and potently toxic (Puddick et al., 2014).

48 MCs have difficulty to penetrate into vertebrate cells via passive transport due to  
49 their hydrophilic nature, and organic anion transporting polypeptides (OATPs) are  
50 known to be able to transport MCs through cell membranes (Campos and Vasconcelos,  
51 2010). Once within the cell, MCs specifically inhibit eukaryotic serine/threonine  
52 protein phosphatases 1 and 2A, which causes the disruption of numerous cellular  
53 signals and processes (Fischer et al., 2005; MacKintosh et al., 1990). Although there  
54 have been 70 members of OATP superfamily identified in the database from humans,  
55 rodents and some additional species (Hagenbuch and Stieger, 2013), not all OATPs  
56 are capable of transporting MCs through cell membranes. The capability of  
57 MC-transport has been demonstrated for OATP1A2 (mainly expressed in the  
58 vertebrate brain), liver-specific OATP1BA and OATP1B3 in humans (Fischer et al.,  
59 2005). In fish, liver-specific OATPs, such as OATP1d1 in little skate (Meier-Abt et al.,  
60 2007) and rtOATP1d1 in rainbow trout (Steiner et al., 2014), have been reported to

61 mediate MC-transport. Different types of OATP distributed in different tissue or  
62 organs possess varying levels of affinities and capacities for different MC variants  
63 (Fischer et al., 2010, 2005; Steiner et al., 2016). Liver is the organ that presents the  
64 highest tropism for MCs (so-called “target”), since it is rich in a few liver-specific  
65 OATP members possessing high affinities and capacities to MCs. Several studies have  
66 reported the acute hepatotoxicity of MCs characterized by hepatocellular apoptosis  
67 (Zhang et al., 2013), necrosis (Mattos et al., 2014), intrahepatic hemorrhaging (Hou et  
68 al., 2015), and cytoskeleton disruption (Zhou et al., 2015). Additionally, the  
69 distribution of MCs in the liver has been detected using immunohistochemical  
70 methods in mice (Guzman and Solter, 2002; Yoshida et al., 1998) and fish (Djediat et  
71 al., 2011; Fischer and Dietrich, 2000; Marie et al., 2012).

72 In addition to liver, MCs have been documented to distribute and accumulate in  
73 various fish organs including intestine, kidney, gill and gonad (Acuña et al., 2012;  
74 Djediat et al., 2010; Mezhoud et al., 2008; Trinchet et al., 2013, 2011). Among these  
75 organs, the gonad could be considered as a secondarily most important target of MCs,  
76 as several field studies reported the presence of MCs in the gonad of fish. For instance,  
77 in Lake Pamvotis (Greece), the gonad of common carp (*Cyprinus caprio*) was  
78 reported to contain about 50 ng eq. MC-LR g<sup>-1</sup> body weight (bw) using the  
79 enzyme-linked immunosorbent assay (ELISA) (Papadimitriou et al., 2012), and in  
80 Lake Taihu (China), three variants of MC (MC-LR, -YR and -LR) were determined in  
81 the gonad of various fish species using a liquid chromatography-electrospray  
82 ionization-mass spectrum system (LC-ESI-MS). Particularly, silver carp  
83 (*Hypophthalmichthys molitrix*) and goldfish (*Carassius auratus*) were observed to  
84 contain high concentrations of MCs in the gonad (60 and 150 ng MCs g<sup>-1</sup> DW,  
85 respectively) (Chen et al., 2009). In laboratories, the distribution of MC-LR in the  
86 gonad of medaka fish administered with pure toxin was also testified using a  
87 radiotracing method (Mezhoud et al., 2008). Although the accumulation of MCs in the  
88 gonad has been documented previously through different methods, little is known  
89 about the localization of MCs within the gonad tissue, or about the intracellular  
90 distribution of MCs. Only one field study reported the presence of MCs in the gonadal

91 somatic tissue, but apparently not in the oocytes in common bream (*Abramis brama*)  
92 using immunohistochemical method (Trinchet et al., 2013). To date, it is still hard to  
93 know whether MC could enter the reproductive cells or only accumulate in the  
94 conjunctive tissue of gonad. Although not the most sensitive detection method, the  
95 immunohistochemical examination is a well-established way of providing the precise  
96 subcellular localization of MCs in the gonad, which could largely advance our current  
97 knowledge of the directly toxic effects of MCs on the gonad.

98 In the present study, in order to investigate subcellular distribution of MCs in fish  
99 gonads, an immunohistochemical assay with light microscopy and electron  
100 microscopy was conducted in adult medaka fish that were gavaged with acute doses  
101 of MC-LR (10  $\mu\text{g}\cdot\text{g}^{-1}$  bw of MC-LR, 1 h exposure). Localization of the toxin in the  
102 gonad was shown by MC-LR-specific antibody, MC10E7, which specifically binds to  
103 the arginine at position 4 of MC-LR (Zeck et al., 2001). In addition, the toxin  
104 distribution and histological change in the liver (the first target of MCs) were also  
105 investigated in order to compare the toxic effect in liver and gonad.

106

## 107 **2. Materials and methods**

### 108 **2.1 Chemical and reagent**

109 MC-LR, purchased from Novakit® (Nantes, France), was selected as the model  
110 MC for the present experiment. 500 hundred  $\mu\text{g}$  of MC-LR was dissolved in 500  $\mu\text{L}$   
111 of ethanol and 500  $\mu\text{L}$  of water. The ethanol was evaporated with a Speedvac. The  
112 concentration of MC-LR in the obtained solution was quantified using a commercial  
113 Adda-specific AD4G2 ELISA test (Abraxis), and then adjusted to be 1  $\mu\text{g}\cdot\mu\text{L}^{-1}$ .

### 114 **2.2 Fish maintenance, exposure and sampling**

115 The experimental procedures were conducted in accordance with the European  
116 Communities Council Directive of 24 November 1986 (86/609/EEC) and the  
117 supervision of the Cuvier's ethical committee of the Museum National d'Histoire  
118 Naturelle (MNHN) concerning the protection of experimental animals.  
119 Five-month-old medaka fish (*Oryzias latipes*) of the inbred Cab strain maintained in  
120 the lab was used for this experiment. Female and male fish were maintained in 2 glass

121 aquaria, respectively, filled with a mixture of tap water and reverse osmosis filtered  
122 water (1:2) in a flow-through system for aeration and filtration, in a temperature  
123 controlled room ( $25 \pm 1$  °C), with a 12 h:12 h light:dark cycle. Fish were fed three  
124 times a day with commercial dry bait for juvenile salmon.

125 Eight females and eight males were randomly selected from the aquaria. The fish  
126 were anesthetized with tricaine ( $150 \text{ mg.L}^{-1}$ ) before gavage. Five females and five  
127 males were gavaged with  $5 \mu\text{L}$  of MC-LR solution ( $1 \mu\text{g}.\mu\text{L}^{-1}$ ) per fish, representing  
128 about  $10 \mu\text{g.g}^{-1}$  bw of MC-LR (average body weight is 0.52 g, the body weight of  
129 individual fish is shown in Supplementary Table). This dose is modified according to  
130 a few previous studies in which medaka fish exhibited noticeable tissue damage and  
131 toxin presence in liver upon exposure to  $5 \mu\text{g.g}^{-1}$  bw of MC-LR (Djediat et al., 2011,  
132 2010). Two females and two males were gavaged with  $5 \mu\text{L}$  water as the non-toxin  
133 control, and 1 female and 1 male without any treatment were used as the non-gavage  
134 control. After 1 h oral exposure, fish were anesthetized with tricaine, sacrificed, and  
135 the liver and gonad were collected on ice. One tissue was cut into 2 parts, one part  
136 was immediately fixed with formaldehyde fixing solution (Supplemental material 1)  
137 according to the protocol provided by the histopathological platform of Ecole  
138 Nationale Vétérinaire d'Alfort (ENVA), and the other part was fixed with  
139 paraformaldehyde fixing solution (Supplemental material 2) following the instruction  
140 of the electron microscopy platform of Muséum National d'Histoire Naturelle  
141 (MNHN).

### 142 **2.3 Histological observation and immunolocalization of microcystins**

143 In the platform of ENVA, the liver and gonad samples fixed in formaldehyde  
144 fixing solution at  $4$  °C for 48 h were dehydrated in successive baths of ethanol (from  
145 70 to 100%) and embedded in paraffin. Blocks were cut into  $4 \mu\text{m}$  thick sections.  
146 Histology was observed with Hematoxylin-Eosin-Saffron (HES) staining (data not  
147 shown). Assessment of hepatic glycogen reserve was evaluated with Periodic  
148 Acid-Schiff (PAS) staining. The glycogen reserve analysis performed by ImageJ  
149 software (version 1.51d) estimated the hepatic glycogen quantity as a surface  
150 percentage of the purple-red pixels on 5 randomly selected photos ( $200 \times$

151 magnification, photo size 1388×1040 pixels, as seen in Figure 1) per individual. For  
152 immunolocalization of MC, sections were incubated with a monoclonal antibody to  
153 MC-LR (MC10E7, Alexis) that recognizes all MCs with Arg in position 4 (dilution  
154 1:4000). The immunolabeling was routinely performed with an automated Module  
155 Discovery XT (Ventana, Tuscon, USA) using a colorimetric peroxidase-specific  
156 staining with diaminobenzidine (DAB), a substrate that produces a highly insoluble  
157 brown precipitate. The slides were counterstained with hematoxylin in the end.  
158 Negative control slides were prepared by skipping the first antibody MC10E7  
159 incubation step. One MC-contaminated medaka liver sample from an acute high dose  
160 exposure in the lab previously was included as the technically positive control.

161 In the platform of MNHN, the liver and gonad samples fixed in  
162 paraformaldehyde fixing solution at 4 °C overnight were dehydrated in successive  
163 baths of ethanol (from 30 to 100%) and embedded into the Unicryl resin. Blocks were  
164 cut into 0.5 µm-thick semi-thin sections (stained with toluidine blue staining) and 60  
165 nm-thick ultrathin sections for histological observation and immunolocalization of  
166 MC with electron microscopy, respectively. The 60 nm-thick ultrathin sections were  
167 collected by gold grids. Then, the sections were incubated with the same primary  
168 antibody (MC10E7) at 4 °C overnight and rinsed, then incubated with a secondary  
169 antibody coupled to gold nanoballs (6 or 10 nm of diameter) at room temperature for  
170 1 h. Negative control slides were prepared by skipping the first antibody MC10E7  
171 incubation step. After being well rinsed with distilled water, the sections were stained  
172 with a saturated solution of uranyl acetate in 50% ethanol and then observed under an  
173 H-7700 Hitachi (Tokyo, Japan) transmission electron microscope.

174

### 175 **3. Results**

176 During the 1 hour of post-gavage, all MC-treated fish exhibit abnormal  
177 swimming behaviors, such as difficulty in moving or losing body balance. In the  
178 contrary, the fish of control group all swim normally. Histological and  
179 immunohistochemical observation results of each individual are summarized in Table  
180 1, which shows visible toxic effects and clear toxin distribution in nearly every

181 MC-treated fish, but not in any control fish.

182 (Table 1)

183

### 184 **3.1 Histological effects with light microscopy**

185 In the liver of all control fish, hepatocytes present compact and characteristic  
186 cord-like parenchymal organization and a distinctive central nucleus with a prominent  
187 nucleolus (Figure 1 A and B). The cytoplasm of hepatocytes contains mainly  
188 glycoprotein and/or glycogen stores that are intensively stained in red-purple with  
189 PAS staining (Figure 1 E and F). In contrast, the livers of MC-LR treated fish exhibit  
190 noticeable tissue lesions characterized by disintegration of the parenchymal  
191 organization and significant cell lysis. The hepatocytes all lose their polyhedral shape  
192 and become rounded and swollen. Within the hepatocytes, the reserve vesicles  
193 disappear, the cytoplasm presents various small bubble-like structures, and the nuclear  
194 chromatin becomes dense. Some hepatocytes exhibit breakdown of the nuclear  
195 membrane, mitosis arrest, and dilation of endoplasmic reticulum (Figure 1 C and D).  
196 In addition, the hepatic intracellular glycoprotein and/or glycogen quantity seems to  
197 decrease, and the mean  $\pm$  standard deviation (SD) values of glycogen percentage for  
198 female controls, male controls, female toxin-treated fish and male toxin-treated fish  
199 are  $15\% \pm 9\%$ ,  $11\% \pm 11\%$ ,  $40\% \pm 16\%$  and  $29\% \pm 16\%$ .

200 For the gonad, there is no apparent cellular difference between the toxin-treated  
201 fish and the control ones.

202 (Figure 1)

### 203 **3.2 Immunolocalization of MC-LR in the liver and the gonad**

204 Through light microscopy, all livers of MC-LR treated fish exhibit a strong  
205 positive signal of MC-LR specific antibodies (Figure 2 B) whereas the negative  
206 control slide does not display any positive signal (Figure 2 C), being similar to control  
207 fish in which no immunolabeling is observed (Figure 2 A). For the toxin treated fish,  
208 the brown immunolabelings are evenly distributed in hepatocytes, but not in blood  
209 cells which are only stained in blue by hematoxylin. Within hepatocytes, the  
210 immunolabeling of MCs is showed in the cytoplasm and more intense labeling is

211 observed in nuclei (Figure 2 B). Immunogold electron microscopy also shows that the  
212 black nanoballs (immunolabelings) are localized in the cytoplasmic inclusion and the  
213 nucleus (Figure 3 C) of hepatocytes of MC-LR treated fish, being particularly intense  
214 in the lysis area (Figure 3 B). MC-LR is also distributed intensely in residual bodies  
215 of the macrophage (Figure 3 D), whereas no immunolabeling is observed in the  
216 control fish (Figure 3 A) or in the negative control slide (Supplementary Figure A and  
217 B).

218 By light microscopy observation of the ovary of toxin-treated fish, clear  
219 immunolabelings are detected in the connective tissue and some round cells with  
220 above 10  $\mu\text{m}$  in diameter, being probably the early stage of oocyte (Figure 2 E),  
221 whereas the negative control slide does not display any positive signal (Figure 2 F),  
222 being similar to the control fish in which no immunolabeling is observed (Figure 2 D).  
223 Moreover, electron microscopy shows that immunogold labelings are not only present  
224 in the gonadal somatic cells, but also distributed intensively in the chorion of oocytes  
225 (Figure 3 G), being less intense in the yolk vesicles and cytoplasm of oocytes (Figure  
226 3 H), whereas no immunolabeling is observed in either the control fish (Figure 3 E  
227 and F) or the negative control slide (Supplementary Figure C).

228 On the light microscope, weaker immunolabelings are found in the testicular  
229 connective tissue of a few toxin-treated male fish (Figure 2 H), whereas the negative  
230 control slide does not display any positive signal (Figure 2 I), being similar to the  
231 control fish in which no immunolabeling is observed (Figure 2 G). Immunogold  
232 electron microscopy shows a remarkable labeling in some round unidentified  
233 structures, being probably some degenerated germ cells (Figure 3 J), as well as in the  
234 connective tissue of certain area nearby seminiferous tubules (Figure 3 K), whereas  
235 no immunolabeling is observed in either the control fish (Figure 3 I) or the negative  
236 control slides (Supplementary Figure D).

237 (Figure 2 and 3)

#### 238 **4. Discussion**

239 MC-treated female and male fish in this study show the characteristic  
240 hepatocellular changes and the depletion of glycogen reserve that have been observed  
241 previously in fish (Djediat et al., 2011; Fischer et al., 2000; Fischer and Dietrich, 2000;  
242 Marie et al., 2012; Mezhoud et al., 2008) and mice (Guzman and Solter, 2002;  
243 Yoshida et al., 2001, 1998) acutely administered with MCs or MC-containing  
244 cyanobacteria extracts. In fact, the observed liver damage in the present study is also  
245 similar to some of those described in the fish after chronic intoxication with MCs  
246 (Acuña et al., 2012; Qiao et al., 2016a; Trinchet et al., 2011). Trinchet and her  
247 colleagues observed an increase in rough endoplasmic reticulum in hepatocytes of  
248 medaka fish chronically exposed to MC-LR ( $5 \mu\text{g.L}^{-1}$ , 30 d), which is also found in  
249 the male toxin-treated medaka in the present study. This could be associated with the  
250 induction of detoxification process. Another chronic in-house study reported a  
251 noticeable hepatic glycogen store depletion in medaka fish upon exposure to MC-LR  
252 ( $5 \mu\text{g.L}^{-1}$ , 28 d) (Qiao et al., 2016a), which is consistent with the acute intoxication  
253 effect of MC-LR observed here, and the increased energy needs for the MC  
254 detoxification process might be the cause.

255 Severe liver damages are often accompanied by remarkable accumulation of MCs  
256 in the liver. The present study shows an intense distribution of MC-LR in the lytic  
257 hepatocyte of the toxin-treated medaka fish through the immunohistochemistry. MCs  
258 have been reported to mostly localize in the cytoplasm of hepatocytes where they  
259 disturb a sequence of phosphorylation/dephosphorylation-dependent biochemical  
260 reactions, resulting in the disruption of multiple cellular processes, and consequently  
261 causing the deformation of hepatocytes, apoptosis and lysis (Campos and  
262 Vasconcelos, 2010). Furthermore, a high concentration of MC-LR is also observed in  
263 the hepatic nucleus here, which is consistent with the results provided in a few  
264 previous acute studies (Fischer et al., 2000; Guzman and Solter, 2002; Yoshida et al.,  
265 1998). Protein phosphatases PP1 and PP2A, one of the main molecular “target” of  
266 MCs, localize in both nucleus and cytoplasm (Shenolikar, 1994). Therefore, the

267 observed nuclear accumulation of MC-LR could be the consequence of the MC  
268 specific antibodies binding to the MC-LR-PP1/PP2A adducts localized in the nucleus.

269 In the present study, MC-LR is also observed to be present in the gonad of  
270 MC-treated fish. For females, MC-LR is localized in the connective tissue of ovary, as  
271 well as in some immature and maturing oocytes. The presence of MC in the connective  
272 tissue of fish ovary has been reported previously in common bream collected from  
273 MC-contaminated lakes (Trinchet et al., 2013). It seems that MCs are transported  
274 through the bloodstream into gonads, in which they can firstly accumulate in the  
275 connective tissue, and then transported into various gonadal somatic cells, even  
276 reproductive cells. Our results indeed exhibit an apparent distribution of MC-LR in  
277 the oocyte of vertebrates with *in vivo* condition for the first time, and the toxin is clearly  
278 localized in the yolk and the cytoplasm of the oocyte, being particularly highly  
279 intensive in the chorion. Recently, one field study detected noticeable microcystin  
280 variants in the egg-shell membranes and yolk of dead hatchlings of Nile crocodiles  
281 (*Crocodylus niloticus*) by using liquid chromatography-high resolution mass  
282 spectrometry (Singo et al., 2017). Through the immunochemistry, MC was once  
283 reported to be present in the oocyte of snail upon exposure to MC-LR for 5 weeks  
284 (Lance et al., 2010). It is unclear how MC-LR enters into oocytes since the oocyte  
285 plasma membrane seems to lack the OATPs possessing MC-transport capability. It  
286 can be assumed that MCs may be transported into oocytes as protein-bound forms  
287 along with protein import during oogenesis, since the exchange of a big amount of  
288 protein and other materials are occurring prior to complete chorion maturation.

289 For MC-treated male fish, immunogold electron microscopy reveals an intense  
290 distribution of MC-LR in the connective tissue of the testis in some certain area, as  
291 well as in some degenerated spermatocyte-like structure, which implies a potential  
292 germ cell damage induced by MC exposure. The connective tissue of the testis  
293 consists of massive fibers and various types of gonadal somatic cells, such as Leydig  
294 cells and Sertoli cells. They are important functional cells in the testis, being  
295 responsible for synthesizing and secreting androgens or transporting of nutrients into

296 the growing germ cells (Dietrich and Krieger, 2009). Therefore, the high  
297 accumulation of MC-LR in the connective tissue and its subsequent toxic effect on  
298 gonadal somatic cells may indirectly disturb spermatogenesis process, affecting the  
299 reproductive process. Although Sertoli cell contributes to the formation of the  
300 blood-testis barrier (BTB) which hinders the diffusion of MCs into the spermatogenic  
301 microenvironment (Wan et al., 2013), a recent *in vitro* study reported that MC-LR can  
302 cause disruption of the tight junction between Sertoli cells, and destroy BTB (Chen et  
303 al., 2018, 2016), implying that MC-LR could enter the spermatogenic  
304 microenvironment and subsequently induce apoptosis and degeneration in the  
305 spermatocyte. This could be one explanation for the accumulation of MC-LR in some  
306 degenerated spermatocyte-like structure observed here. Considerable testicular injury  
307 and spermatocyte abnormality have been found in several species of vertebrate model  
308 animals, such as mouse, rat and fish, upon exposure to MCs acutely or chronically (Li  
309 et al., 2008; Su et al., 2016; X. Wang et al., 2013; Zhao et al., 2012; Zhou et al., 2013).  
310 However, to date, according to *in vivo* studies using these vertebrate models, no  
311 evidence regarding the incorporation of MCs into spermatocytes has been reported yet.  
312 In the present study, MC-LR is not found in any clear spermatocytes of the  
313 toxin-treated fish through the immunogold labeling technique, which is attributed to  
314 the integrity of BTB and the organ distribution of the MC-transporting OATPs. The  
315 identified OATPs that possess strong MC-transport capabilities are highly abundant in  
316 the liver, but hardly known to be present in the cell membrane of reproductive cells  
317 (Ho and Kim, 2018). However, two *in vitro* studies reported that MC-LR was able to  
318 immigrate into isolated rat spermatogonia (L. Wang et al., 2013; Zhou et al., 2012).  
319 Furthermore, in Zhou's study, at least 5 OATPs were detected at the mRNA level in  
320 spermatogonia and their expression level was affected by MC-LR, implying that these  
321 OATPs may involve in MC-transport into male reproductive cells. It seems that some  
322 unidentified OATPs which possess MC-transport capabilities might be expressed in  
323 male reproductive cells at a relatively low level. But the information regarding the  
324 unidentified MC-transporting OATPs and their expression level on germ cells remains  
325 very limited. Due to various physiological differences between female and male fish

326 (Qiao et al., 2016b), the toxic effects of MC on gonads of two genders of fish seem to  
327 be different. One previous study demonstrated that female zebrafish are more  
328 vulnerable than males to MC-LR exposure indicated by more cell apoptosis in ovary  
329 compared with testis (Qiao et al., 2013). The present study also showed a clear  
330 accumulation of MC in oocytes but not spermatocytes with *in vivo* condition, which  
331 implies a consistent idea that MC exposure exerts more potent reprotoxic effects on  
332 female fish than males.

333 It is worth to mention that the process of histological section preparation may  
334 affect the result, since a fraction of MC-LR (mainly free MC-LR) can be removed  
335 during the dehydrating process of the section preparation. The immunostaining here  
336 indeed detects MC-LR-PP1/PP2A adducts mostly, due to the strong affinity of  
337 MC-LR to protein phosphatases PP1/PP2A (Yoshida et al., 2001). Dmet-Asp and  
338 D-Glu residues of MC-LR play important roles in forming the MC-LR-PP1/PP2A  
339 adducts (Campos and Vasconcelos, 2010). Nevertheless, the present acute study  
340 indeed shows a clear subcellular distribution of MC-LR in the gonad of the  
341 toxin-treated fish, implying a direct effect of gonadal impairment on reproductive  
342 function. However, in another in-house chronic study, MCs were not detected in the  
343 ovary or testis of medaka fish following a balneation exposure to 5  $\mu\text{g}\cdot\text{L}^{-1}$  of MC-LR  
344 for 30 days using the same immunolocalization techniques (Qiao et al., 2016a), which  
345 suggests a more potent and indirect effect of liver dysfunction on fish reproduction  
346 upon chronic low-dose exposure. Comparing these two studies, toxin concentration,  
347 and exposure time account for the discrepancy. In the present study, 10  $\mu\text{g}\cdot\text{g}^{-1}$  bw of  
348 MC-LR is a quite high concentration (LD<sub>50</sub> values of MC-LR by i.p. injection range  
349 from 50 to 400  $\mu\text{g}\cdot\text{kg}^{-1}$  bw in different species of fish) (Testai et al., 2016), and the  
350 short time of exposure (1 h) largely reduced the possible toxin excretion process  
351 through liver detoxification, together leading to a sufficient quantity of toxin that  
352 could access to gonad through blood stream and be detected by the  
353 immunohistological method.

354

355 **5. Conclusion**

356 Our histological and immunohistochemical results reveal that both liver and  
357 gonad are significantly affected by MC-LR exposure. An intense distribution of  
358 MC-LR within hepatocytes along with a severe liver damage attests to the potent  
359 hepatotoxicity of MC. The immunohistochemical results show that, besides being  
360 accumulated in the hepatocytes, MC-LR is also found in the connective tissue of the  
361 gonads, as well as in the reproductive cells (oocytes but not spermatocytes). This  
362 finding constitutes the first observation of the presence of MC in the reproductive  
363 cells (female, oocytes) in vertebrate model animals with *in vivo* condition. Both liver  
364 and gonad play important roles in the reproductive process of oviparous vertebrates.  
365 Our results of the present acute study, which provide a distinct subcellular localization  
366 of MC-LR in the liver and gonad, contributes to a better understanding of the  
367 potential reproductive toxicity of MC-LR at the histological level, favoring the  
368 characterization of underlying mechanisms. Meanwhile, the penetration of MCs into  
369 the reproductive cell suggests a possible transferring of MCs from adults into  
370 offspring which could cause a big issue for the population of aquatic organisms. The  
371 further investigation concerning this perspective is needed to advance our current  
372 knowledge of the protection of aquatic organism populations, as well as human beings  
373 from the widespread MCs in the freshwater body.

374

375 **Acknowledgments**

376 This work was supported by grants from the CNRS Défi ENVIROMICS  
377 “Toxycyfish” project and from the ATM “Cycles biologiques: evolution et adaptation”  
378 of the MNHN to Dr. Benjamin Marie. Qin Qiao Ph.D. is founded by the China  
379 Scholarship Council. We thank the Amagen platform for providing medaka fish Cab  
380 strain, the microscopy platform of ENVA and MNHN for the histology and  
381 immunolocalization techniques. We also thank Marie-Claude Mercier for its  
382 administrative support.

383 **Author Contribution**

384 Q.Q., C.D., H.H., C.B., M.E. and B.M. conceived the experiments, Q.Q., C.D., H.H,  
385 C.D., S.L.M. and B.M. conducted the experiments, Q.Q., C.D., H.H and B.M.  
386 analyzed the results. All authors reviewed the manuscript.

387 The authors declare no competing financial interest.

388

389 **List of Supplementary materials:**

390 Supplementary material 1. Formaldehyde fixing solution (100 mL) provided by the  
391 platform of ENVA

392 Supplementary material 2. Paraformaldehyde fixing solution (100 mL) provided by the  
393 platform of MNHN

394 Supplementary Table. The body weight of individual fish in different treatment groups

395 Supplementary Figure. Representative photos of the negative control slide for the  
396 liver and gonad of toxin-treated fish through immunogold electron microscopy.

397

398 **Figure descriptions:**

399 Figure 1. Representative photos of histological observation of medaka liver under a  
400 light microscope.

401 A-D: resin sections (0.5  $\mu\text{m}$  thick) of medaka liver with toluidine blue staining.

402 Female controls (A): abundant and distinct distribution of reserve vesicles (v);

403 Females exposed to 10  $\mu\text{g}\cdot\text{g}^{-1}$  bw of MC-LR (C): disintegration of the cord-like

404 parenchymal organization, rounded hepatocytes containing various small bubbles (b),

405 loss of reserve vesicles, nuclear membrane breakdown, chromatin concentration (c);

406 Male controls (B): abundant and distinct distribution of reserve vesicles (v); Males

407 exposed to 10  $\mu\text{g}\cdot\text{g}^{-1}$  bw of MC-LR (D): disintegration of the cord-like parenchymal

408 organization, swollen and rounded hepatocytes, nuclear chromatin condensation (c),

409 and dilation in endoplasmic reticulum (e) and loss of nuclei (n). E-H: paraffin sections

410 (4  $\mu\text{m}$  thick) of medaka liver with PAS staining. Female (E) and male (F) controls:

411 abundant and distinct distribution of glycogen-reserve vesicles (red-purple); Females

412 (G) and males (H) exposed to 10  $\mu\text{g}\cdot\text{g}^{-1}$  bw of MC-LR: less glycogen-reserve vesicles

413 compared with the control group.

414

415 Figure 2. Representative photos of immunolocalization of MC-LR in the liver and  
416 gonad of toxin-treated fish through light microscopy.

417 The liver (A), ovary (D), and testis (G) of control fish incubated with MC-LR  
418 immunolabeling (MC10E7): no immunolabeling. The liver (B), ovary (E), and testis  
419 (H) of the fish exposed to  $10 \mu\text{g}\cdot\text{g}^{-1}$  bw of MC-LR incubated with MC-LR  
420 immunolabeling (MC10E7), and revealed with peroxidase specific reaction of DAB.

421 For the liver, brown labelings of MC-LR are found in the cytoplasm and nuclei (n) of  
422 hepatocytes, but not in the blood cell (h); For the ovary, brown labelings of MC-LR  
423 are detected in the connective tissue and some round cells; For the testis,  
424 immunolabelings are observed in the testicular connective tissue. The negative control  
425 slides of the toxin-treated liver (C), ovary (F), and testis (I) incubated with only the  
426 secondary antibody: no immunolabeling.

427

428 Figure 3. Representative photos of immunolocalization of MC-LR in the liver and  
429 gonad of toxin-treated fish through immunogold electron microscopy.

430 The liver (A), ovary (E and F) and testis (I) of control fish: no clear immunolabeling.

431 The liver (B-D), ovary (G-H) and testis (J and K) of the fish exposed to  $10 \mu\text{g}\cdot\text{g}^{-1}$  bw  
432 of MC-LR, showing the immunolabeling of MC-LR indicated by the white arrow. For

433 the liver, immunolabelings of MC-LR are clearly observed in the lytic residual (B)

434 and nuclear (C) of hepatocyte and the macrophage (D), particularly in the residual

435 bodies (r); For the ovary, immunolabelings are found in the connective tissue (left)

436 and the chorion (c) of the oocyte (G, right), and less labelings are observed in the yolk

437 vesicle (y) and the cytoplasm (cy) of the oocyte (H). For the testis, labelings are

438 intensively distributed in some degenerated germ cell-like structures (J), and in the

439 connective tissue of certain area nearby seminiferous tubules (K).

440

## 441 **Reference**

442 Acuña, S., Baxa, D., Teh, S., 2012. Sublethal dietary effects of microcystin producing

443 *Microcystis* on threadfin shad, *Dorosoma petenense*. *Toxicon* 60, 1191–1202.  
444 doi:10.1016/j.toxicon.2012.08.004

445 Campos, A., Vasconcelos, V., 2010. Molecular mechanisms of microcystin toxicity in  
446 animal cells. *Int. J. Mol. Sci.* 11, 268–287. doi:10.3390/ijms11010268

447 Chen, J., Zhang, D., Xie, P., Wang, Q., Ma, Z., 2009. Simultaneous determination of  
448 microcystin contaminations in various vertebrates (fish, turtle, duck and water  
449 bird) from a large eutrophic Chinese lake, Lake Taihu, with toxic *Microcystis*  
450 blooms. *Sci. Total Environ.* 407, 3317–3322.  
451 doi:10.1016/j.scitotenv.2009.02.005

452 Chen, Y., Wang, J., Pan, C., Li, D., Han, X., 2018. Microcystin–leucine–arginine  
453 causes blood–testis barrier disruption and degradation of occludin mediated by  
454 matrix metalloproteinase-8. *Cell. Mol. Life Sci.* 75, 1117–1132.  
455 doi:10.1007/s00018-017-2687-6

456 Chen, Y., Zhou, Y., Wang, J., Wang, L., Xiang, Z., Li, D., Han, X., 2016.  
457 Microcystin-leucine arginine causes cytotoxic effects in Sertoli cells resulting in  
458 reproductive dysfunction in Male Mice. *Sci. Rep.* 6, 1–18.  
459 doi:10.1038/srep39238

460 Dietrich, D.R., Krieger, H.O., 2009. Chapter 5. Male gonad anatomy and morphology,  
461 in: *Histological Analysis of Endocrine-Disruptive Effects in Small Laboratory*  
462 *Fish*. pp. 88–114.

463 Djediat, C., Malécot, M., de Luze, A., Bernard, C., Puiseux-Dao, S., Edery, M., 2010.  
464 Localization of microcystin-LR in medaka fish tissues after cyanotoxin gavage.  
465 *Toxicon* 55, 531–535. doi:10.1016/j.toxicon.2009.10.005

466 Djediat, C., Moyenga, D., Malécot, M., Comte, K., Yéprémian, C., Bernard, C.,  
467 Puiseux-Dao, S., Edery, M., 2011. Oral toxicity of extracts of the  
468 microcystin-containing cyanobacterium *Planktothrix agardhii* to the medaka fish  
469 (*Oryzias latipes*). *Toxicon* 58, 112–122. doi:10.1016/j.toxicon.2011.05.011

470 Fischer, A., Hoeger, S.J., Stemmer, K., Feurstein, D.J., Knobeloch, D., Nussler, A.,  
471 Dietrich, D.R., 2010. The role of organic anion transporting polypeptides  
472 (OATPs/*SLCOs*) in the toxicity of different microcystin congeners *in vitro*: A

473 comparison of primary human hepatocytes and OATP-transfected HEK293 cells.  
474 Toxicol. Appl. Pharmacol. 245, 9–20. doi:10.1016/j.taap.2010.02.006

475 Fischer, W.J., Altheimer, S., Cattori, V., Meier, P.J., Dietrich, D.R., Hagenbuch, B.,  
476 2005. Organic anion transporting polypeptides expressed in liver and brain  
477 mediate uptake of microcystin. Toxicol. Appl. Pharmacol. 203, 257–263.  
478 doi:10.1016/j.taap.2004.08.012

479 Fischer, W.J., Dietrich, D.R., 2000. Pathological and biochemical characterization of  
480 microcystin-induced hepatopancreas and kidney damage in carp (*Cyprinus*  
481 *carpio*). Toxicol. Appl. Pharmacol. 164, 73–81. doi:10.1006/taap.1999.8861

482 Fischer, W.J., Hitzfeld, B.C., Tencalla, F., Eriksson, J.E., Mikhailov, A., Dietrich,  
483 D.R., 2000. Microcystin-LR toxicodynamics, induced pathology, and  
484 immunohistochemical localization in livers of blue-green algae exposed rainbow  
485 trout (*oncorhynchus mykiss*). Toxicol. Sci. 54, 365–73.  
486 doi:10.1093/toxsci/54.2.365

487 Guzman, R.E., Solter, P.F., 2002. Characterization of sublethal microcystin-LR  
488 exposure in mice. Vet. Pathol. 39, 17–26. doi:10.1354/vp.39-1-17

489 Hagenbuch, B., Stieger, B., 2013. The SLCO (former SLC21) superfamily of  
490 transporters. Mol. Aspects Med. 34, 396–412. doi:10.1016/j.mam.2012.10.009

491 Ho, R.H., Kim, R.B., 2018. Uptake Transporters, in: Comprehensive Toxicology.  
492 Elsevier, pp. 574–616. doi:10.1016/B978-0-12-801238-3.95625-3

493 Hou, J., Li, L., Xue, T., Long, M., Su, Y., Wu, N., 2015. Hepatic positive and  
494 negative antioxidant responses in zebrafish after intraperitoneal administration of  
495 toxic microcystin-LR. Chemosphere 120, 729–736.  
496 doi:10.1016/j.chemosphere.2014.09.079

497 Lance, E., Josso, C., Dietrich, D., Ernst, B., Paty, C., Senger, F., Bormans, M., Gérard,  
498 C., 2010. Histopathology and microcystin distribution in *Lymnaea stagnalis*  
499 (Gastropoda) following toxic cyanobacterial or dissolved microcystin-LR  
500 exposure 98, 211–220.

501 Li, Y., Sheng, J., Sha, J., Han, X., 2008. The toxic effects of microcystin-LR on the  
502 reproductive system of male rats *in vivo* and *in vitro*. Reprod. Toxicol. 26,

503 239–245. doi:10.1016/j.reprotox.2008.09.004

504 MacKintosh, C., Beattie, K.A., Klumpp, S., Cohen, P., Codd, G.A., 1990.

505 Cyanobacterial microcystin-LR is a potent and specific inhibitor of protein

506 phosphatases 1 and 2A from both mammals and higher plants. FEBS 264,

507 187–192.

508 Marie, B., Huet, H., Marie, A., Djediat, C., Puiseux-Dao, S., Catherine, A., Trinchet,

509 I., Edery, M., 2012. Effects of a toxic cyanobacterial bloom (*Planktothrix*

510 *agardhii*) on fish: Insights from histopathological and quantitative proteomic

511 assessments following the oral exposure of medaka fish (*Oryzias latipes*). Aquat.

512 Toxicol. 114–115, 39–48. doi:10.1016/j.aquatox.2012.02.008

513 Mattos, L.J., Valença, S.S., Azevedo, S.M.F.O., Soares, R.M., 2014. Dualistic

514 evolution of liver damage in mice triggered by a single sublethal exposure to

515 Microcystin-LR. Toxicol. 83, 43–51. doi:10.1016/j.toxicol.2014.02.015

516 Meier-Abt, F., Hammann-Hänni, A., Stieger, B., Ballatori, N., Boyer, J.L., 2007. The

517 organic anion transport polypeptide 1d1 (Oatp1d1) mediates hepatocellular

518 uptake of phalloidin and microcystin into skate liver. Toxicol. Appl. Pharmacol.

519 218, 274–279. doi:10.1016/j.taap.2006.11.015

520 Mezhoud, K., Bauchet, A.L., Château-Joubert, S., Praseuth, D., Marie, A., François,

521 J.C., Fontaine, J.J., Jaeg, J.P., Cravedi, J.P., Puiseux-Dao, S., Edery, M., 2008.

522 Proteomic and phosphoproteomic analysis of cellular responses in medaka fish

523 (*Oryzias latipes*) following oral gavage with microcystin-LR. Toxicol. 51,

524 1431–1439. doi:10.1016/j.toxicol.2008.03.017

525 Papadimitriou, T., Kagalou, I., Stalikas, C., Pilidis, G., Leonardos, I.D., 2012.

526 Assessment of microcystin distribution and biomagnification in tissues of aquatic

527 food web compartments from a shallow lake and evaluation of potential risks to

528 public health. Ecotoxicology 21, 1155–1166. doi:10.1007/s10646-012-0870-y

529 Puddick, J., Prinsep, M.R., Wood, S.A., Kaufononga, S.A.F., Cary, S.C., Hamilton,

530 D.P., 2014. High levels of structural diversity observed in microcystins from

531 *Microcystis* CAWBG11 and characterization of six new microcystin congeners.

532 Mar. Drugs 12, 5372–5395. doi:10.3390/md12115372

533 Qiao, Q., Le Manach, S., Huet, H., Duvernois-Berthet, E., Chaouch, S., Duval, C.,  
534 Sotton, B., Ponger, L., Marie, A., Mathéron, L., Lennon, S., Bolbach, G., Djediat,  
535 C., Bernard, C., Edery, M., Marie, B., 2016a. An integrated omic analysis of  
536 hepatic alteration in medaka fish chronically exposed to cyanotoxins with  
537 possible mechanisms of reproductive toxicity. *Environ. Pollut.* 219, 119–131.  
538 doi:10.1016/j.envpol.2016.10.029

539 Qiao, Q., Le Manach, S., Sotton, B., Huet, H., Duvernois-Berthet, E., Paris, A., Duval,  
540 C., Ponger, L., Marie, A., Blond, A., Mathéron, L., Vinh, J., Bolbach, G., Djediat,  
541 C., Bernard, C., Edery, M., Marie, B., 2016b. Deep sexual dimorphism in adult  
542 medaka fish liver highlighted by multi-omic approach. *Sci. Rep.* 6, 32459.  
543 doi:10.1038/srep32459

544 Qiao, Q., Liu, W., Wu, K., Song, T., Hu, J., Huang, X., Wen, J., Chen, L., Zhang, X.,  
545 2013. Female zebrafish (*Danio rerio*) are more vulnerable than males to  
546 microcystin-LR exposure, without exhibiting estrogenic effects. *Aquat. Toxicol.*  
547 142–143, 272–282. doi:10.1016/j.aquatox.2013.07.002

548 Shenolikar, S., 1994. Protein serine/threonine phosphatases - new avenues for cell  
549 regulation. *Annu. Biol.* 10, 55–86.

550 Singo, A., Myburgh, J.G., Laver, P.N., Venter, E.A., Gezina, C.H., Rösemann, G.M.,  
551 Botha, C.J., 2017. Vertical transmission of microcystins to Nile crocodile  
552 (*Crocodylus niloticus*) eggs. *Toxicon* 134, 50–56.  
553 doi:10.1016/j.toxicon.2017.05.017

554 Spoo, L., Catherine, A., 2017. Appendix 3: Tables of microcystins and nodularins, in:  
555 Handbook of Cyanobacterial Monitoring and Cyanotoxin Analysis. pp. 526–537.  
556 doi:10.1002/9781119068761.app3

557 Steiner, K., Hagenbuch, B., Dietrich, D.R., 2014. Molecular cloning and functional  
558 characterization of a rainbow trout liver Oatp. *Toxicol. Appl. Pharmacol.* 280,  
559 534–542. doi:10.1016/j.taap.2014.08.031

560 Steiner, K., Zimmermann, L., Hagenbuch, B., Dietrich, D., 2016. Zebrafish  
561 Oatp-mediated transport of microcystin congeners. *Arch. Toxicol.* 90,  
562 1129–1139. doi:10.1007/s00204-015-1544-3

563 Su, Y., Li, L., Hou, J., Wu, N., Lin, W., Li, G., 2016. Life-cycle exposure to  
564 microcystin-LR interferes with the reproductive endocrine system of male  
565 zebrafish. *Aquat. Toxicol.* 175, 205–212. doi:10.1016/j.aquatox.2016.03.018

566 Testai, E., Buratti, F.M., Funari, E., Manganelli, M., Vichi, S., Arnich, N., Biré, R.,  
567 Fessard, V., Sialehaamo, A., 2016. Review and analysis of occurrence ,  
568 exposure and toxicity of cyanobacteria toxins in food. *EFSA Support. Publ.*  
569 2016EN-998. 309. doi:10.2903/SP.EFSA.2016.EN-998

570 Trinchet, I., Cadel-Six, S., Djediat, C., Marie, B., Bernard, C., Puiseux-Dao, S., Krysz,  
571 S., Edery, M., 2013. Toxicity of harmful cyanobacterial blooms to bream and  
572 roach. *Toxicol.* 71, 121–127. doi:10.1016/j.toxicol.2013.05.019

573 Wan, H.T., Mruk, D.D., Wong, C.K.C., Cheng, C.Y., 2013. The apical ES-BTB-BM  
574 functional axis is an emerging target for toxicant-induced infertility. *Trends Mol.*  
575 *Med.* 19, 396–405. doi:10.1016/j.molmed.2013.03.006

576 Wang, L., Wang, X., Geng, Z., Zhou, Y., Chen, Y., Wu, J., Han, X., 2013.  
577 Distribution of microcystin-LR to testis of male Sprague-Dawley rats.  
578 *Ecotoxicology* 22, 1555–1563. doi:10.1007/s10646-013-1141-2

579 Wang, X., Chen, Y., Zuo, X., Ding, N., Zeng, H., Zou, X., Han, X., 2013. Microcystin  
580 (-LR) induced testicular cell apoptosis via up-regulating apoptosis-related genes  
581 in vivo. *Food Chem. Toxicol.* 60, 309–317. doi:10.1016/j.fct.2013.07.039

582 Yoshida, T., Makita, Y., Tsutsumi, T., Nagata, S., Tashiro, F., Yoshida, F., Sekijima,  
583 M., Tamura, S., Harada, T., Maita, K., Ueno, Y., 1998. Immunohistochemical  
584 localization of microcystin-LR in the liver of mice: A study on the pathogenesis  
585 of microcystin-LR-induced hepatotoxicity. *Toxicol. Pathol.* 26, 411–418.  
586 doi:10.1177/019262339802600316

587 Yoshida, T., Tsutsumi, T., Nagata, S., Yoshida, F., Maita, K., Harada, T., Ueno, Y.,  
588 2001. Quantitative analysis of intralobular distribution of microcystin-LR in the  
589 mouse liver. *J. Toxicol. Pathol.* 14, 205–212. doi:10.1293/tox.14.205

590 Zeck, A., Eikenberg, A., Weller, M.G., Niessner, R., 2001. Highly sensitive  
591 immunoassay based on a monoclonal antibody specific for [ 4-arginine ]  
592 microcystins. *Anal. Chim. Acta* 441, 1–13.

593 Zhang, H., Cai, C., Fang, W., Wang, J., Zhang, Y., Liu, J., Jia, X., 2013. Oxidative  
594 damage and apoptosis induced by microcystin-LR in the liver of *Rana*  
595 *nigromaculata* in vivo. *Aquat. Toxicol.* 140–141, 11–18.  
596 doi:10.1016/j.aquatox.2013.05.009

597 Zhao, S., Xie, P., Li, G., Jun, C., Cai, Y., Xiong, Q., Zhao, Y., 2012. The proteomic  
598 study on cellular responses of the testes of zebrafish (*Danio rerio*) exposed to  
599 microcystin-RR. *Proteomics* 12, 300–312. doi:10.1002/pmic.201100214

600 Zhou, M., Tu, W.W., Xu, J., 2015. Mechanisms of microcystin-LR-induced  
601 cytoskeletal disruption in animal cells. *Toxicol.* 101, 92–100.  
602 doi:10.1016/j.toxicol.2015.05.005

603 Zhou, Y., Chen, Y., Yuan, M., Xiang, Z., Han, X., 2013. In vivo study on the effects  
604 of microcystin-LR on the apoptosis, proliferation and differentiation of rat  
605 testicular spermatogenic cells of male rats injected i.p. with toxins. *J. Toxicol.*  
606 *Sci.* 38, 661–70. doi:10.2131/jts.38.661

607 Zhou, Y., Yuan, J., Wu, J., Han, X., 2012. The toxic effects of microcystin-LR on rat  
608 spermatogonia *in vitro*. *Toxicol. Lett.* 212, 48–56.  
609 doi:10.1016/j.toxlet.2012.05.001

610

Figure 1

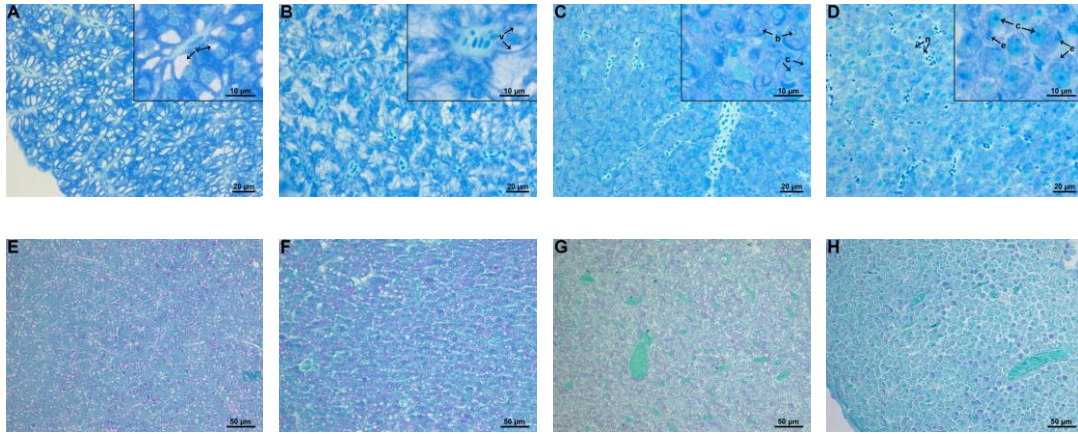


Figure 2

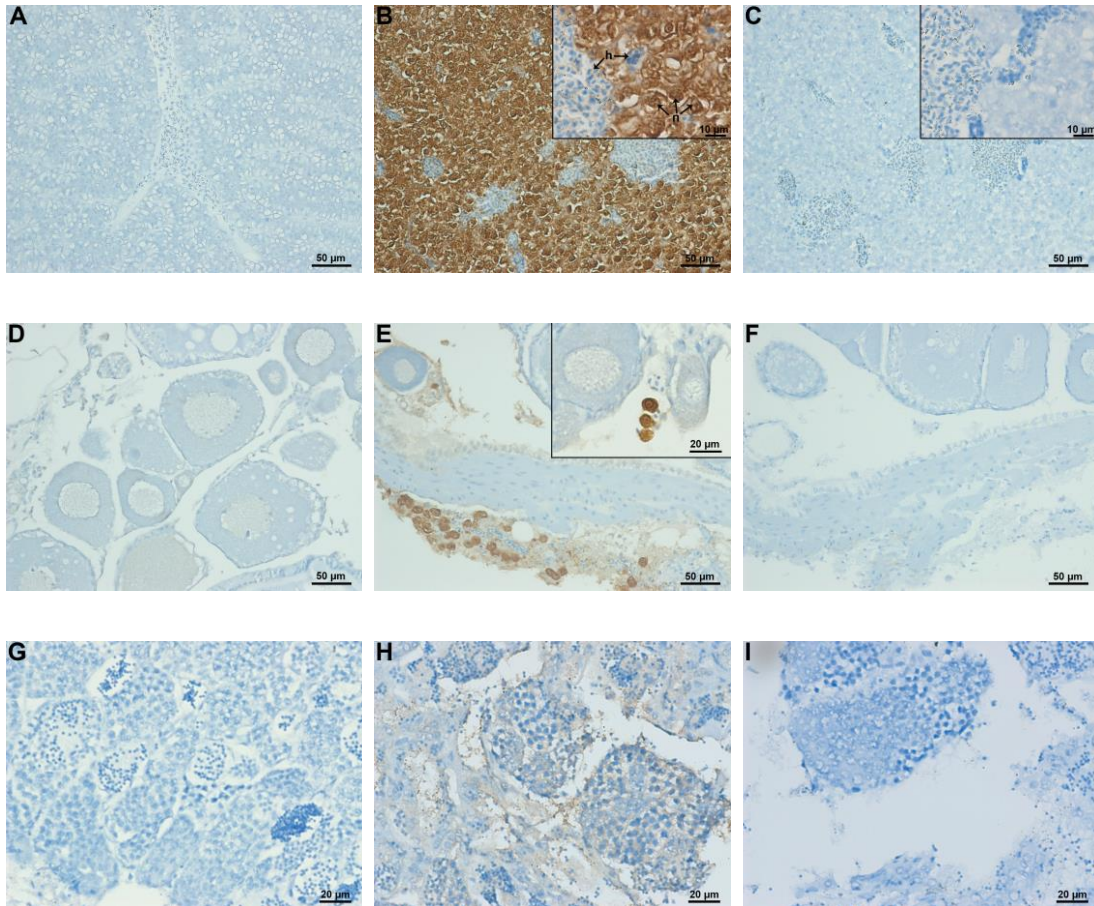
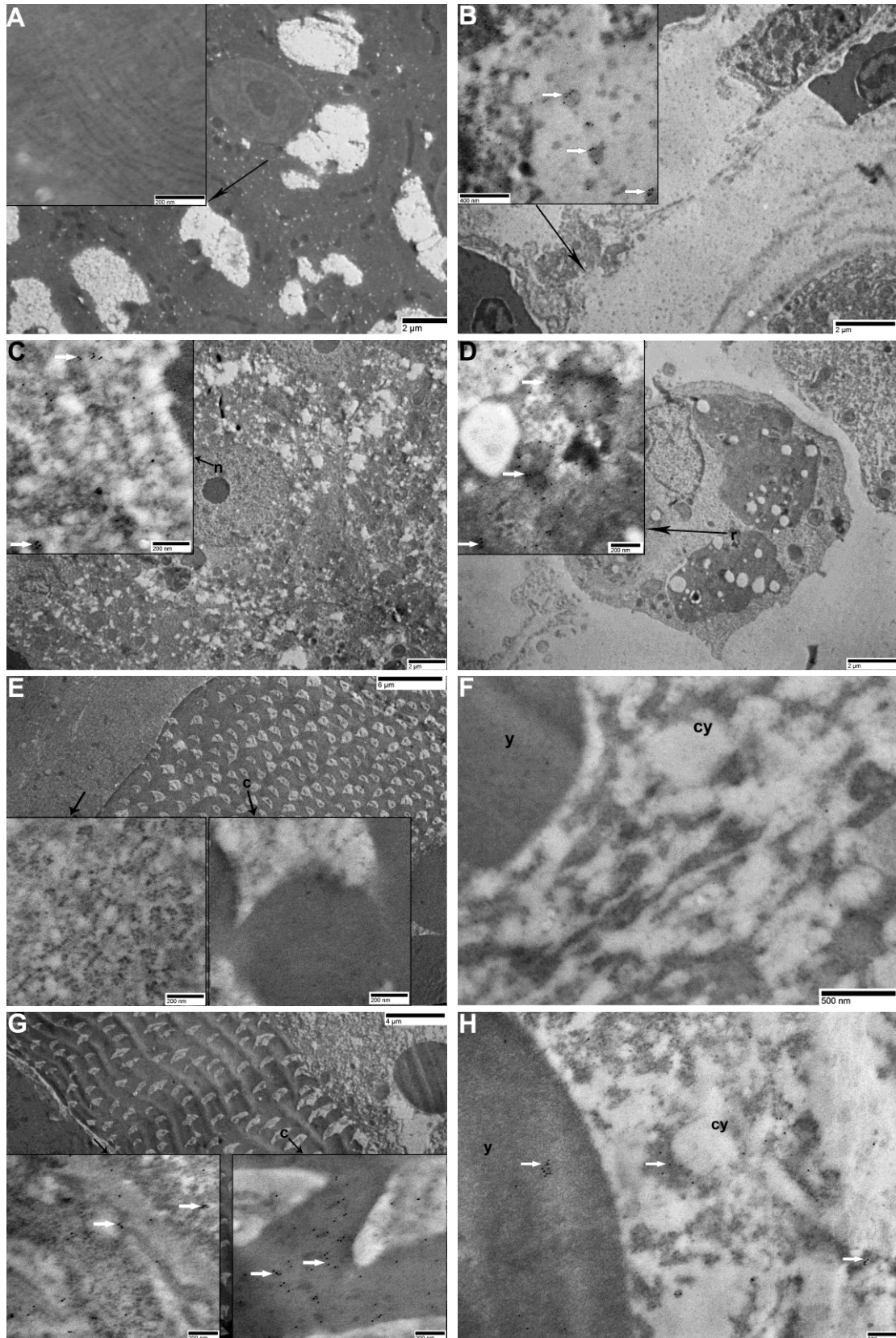


Figure 3



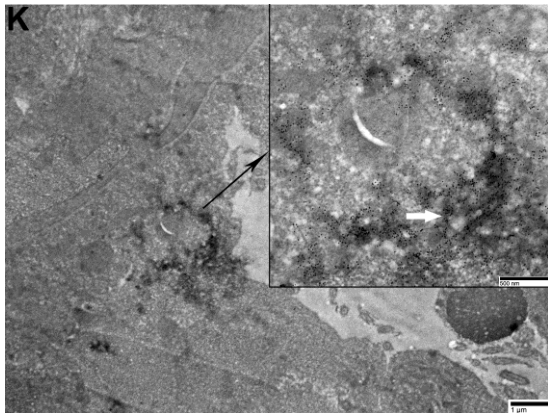
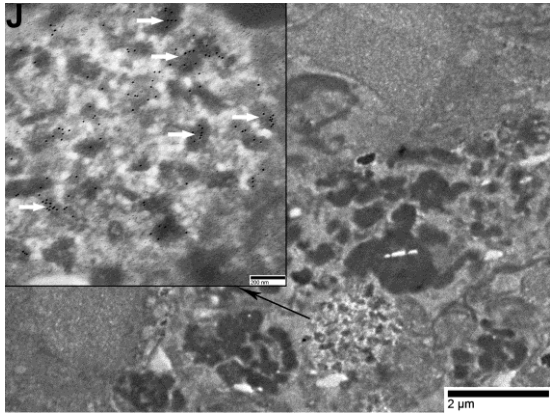
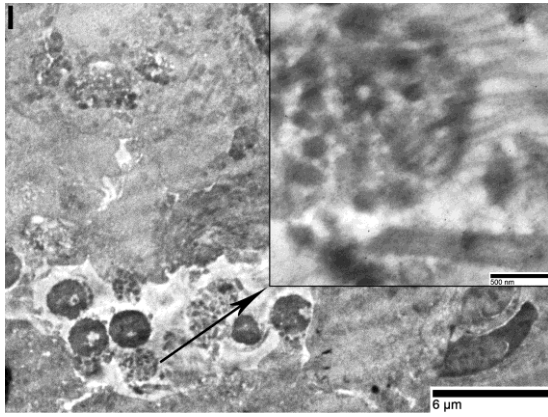


Table 1 Histological and immunohistochemical observation of each individual liver and gonad

Group	Fish <sup>a</sup>	Post-gavage	Histology (Liver)		Anti-MC-LR labeling			
			Light microscopy		Light microscopy <sup>d</sup>		Electron microscopy <sup>e</sup>	
			Liver damage <sup>b</sup>	Glycogen reserve (%) <sup>c</sup>	Liver	Gonad	Gonad	
10 $\mu\text{g}\cdot\text{g}^{-1}$ b.w. of MC-LR	F01	1 h	+	23%	89%	0.1%	++	
	F03	1 h	++	22%	79%	0.1%	+	
	F04	1 h	+	15%	76%	0.2%	++	
	F07	1 h	++	12%	97%	2.9%	++	
	F10	1 h	+	1%	95%	0.5%	n.o.	
	M02	1 h	+	0%	89%	0	++	
	M05	1 h	++	20%	26%	0.1%	++	
	M06	1 h	+	2%	15%	0.1%	n.o.	
	M08	1 h	+	26%	89%	0	+	
M09	1 h	+	6%	89%	0.7%	++		
Control	F12	1 h	0	22%	0	0	0	
	Non-toxin	F14	1 h	0	50%	0	0	0
		M13	1 h	0	16%	0	0	0
		M11	1 h	0	25%	0	0	0
	Non-gavage	F16	1 h	0	49%	0	0	0
		M15	1 h	0	47%	0	0	0

<sup>a</sup> F and M indicate female and male fish, respectively. <sup>b</sup> “++” indicates a severe liver damage, characterized by a large proportion of rounded hepatocytes, significant mitosis arrest, and obvious cell lysis and disjunction. “+” indicates a moderate liver damage, characterized by a large proportion of rounded hepatocytes, and a small area of cell lysis and disjunction. “0” indicates the normal liver structure. <sup>c</sup> indicates the percentage of glycogen reserve in the liver, the calculation formula: the area of the purple-red pixels  $\div$  the area of the whole image (1388 $\times$ 1040 pixels)  $\times$  100%. <sup>d</sup> indicates the percentage of brown immunolabelings in the liver and gonad, the calculation formula: the area of the brown pixels  $\div$  the area of the whole image (1388 $\times$ 1040 pixels)  $\times$  100%. <sup>e</sup> “++” indicates strong and widely distributed immunolabelings, “+” indicates only a few immunolabeling spots, “0” indicates no immunolabeling, and “n.o.” indicates not observed.